

EFFECT OF ANNEALING TEMPERATURE ON THE STRUCTURE, OPTICAL AND ELECTRONIC PROPERTIES OF TiO₂ MADE BY THERMAL TREATMENT OF Ti

DANG TRAN CHIEN

Faculty of Science, Hanoi University of Natural Resources and Environment

PHAM DUY LONG

Institute of Materials Science, Vietnam Academy of Science and Technology

E-mail: dtchien@hunre.edu.vn

Received 24 February 2014

Accepted for publication 04 April 2014

Abstract. *In this work, TiO₂ nanocrystalline thin films were obtained through evaporating Ti films by Electron Beam Deposition (EBD) followed by thermal treatment. The deposition speed of Ti thin films was carried out at 0.15 nm/s and 1 nm/s. The results show that after annealing at 450°C for 8 h, the obtained TiO₂ thin films have nanoparticle structure with grain size of 20 nm for the Ti thin film deposited at the rate of 1nm/s, whereas at the a deposition rate of 0.15 nm/s, the TiO₂ has a nanorod structure with the rod length of 300 – 400 nm. The influence of thermal annealing on structure of TiO₂ films have been investigated and indicated that when annealed at 450°C for 8 hours, all the Ti films were completely oxidized to form TiO₂ films with anatase phase. Whereas, at 700°C the rutile phase was formed. The band gap of TiO₂ thin films decreased with annealing temperature in both doposition rate of Ti thin films. The response of the films annealed at 450°C presented a faster rise and fall in photocurrent under UV illumination on and off interval. Nanoporous structure TiO₂ shows photoelectronic property better than that of nanorod structure. The TiO₂ films were used in a photo-electrochemical (PEC) cell as a working electrode and a platinum electrode as a counter electrode. The electrolyte solution contains 1 M KCl and 0.1 M Na₂S.*

Keywords: TiO₂ thin films, nanoparticle structure, nanorod structure, photo-electrochemical cell.

I. INTRODUCTION

Titanium dioxide is a material which has attracted lots of attention due to its importance in a variety of practical applications. This material is known to exist in several forms, among the most abundant are anatase, rutile and brookite [13]. Anatase TiO₂ films have numerous interesting applications in optical coatings, optical waveguides, photo-decomposition of environmental pollutants, sensing, solar cells and electronic devices, etc [16, 17, 21]. There are numerous reports describing the fabrication of Ti thin films using techniques such as electron beam deposition [7], doctor blading [14], magnetron sputtering [15] sol-gel processing [6], surfactant template self-assembly [1], pulsed laser deposition [3], spray pyrolysis, etc. Among these fabrication methods, the electron beam deposition has many advantages, such as a uniform deposition over a relatively

larger area, the freedom to choose substrate material and strong adhesion to substrate. This work aims to study the effect of annealing temperature on the crystalline structure, optical, and electronic properties of the TiO₂ thin film based Ti films deposited by EBD combined with thermal process.

II. EXPERIMENTAL SETUP

A 300 nm thick layer of Ti was deposited onto various substrates by an electron beam with 6 keV of energy at 10⁻⁵ torr pressure. The deposition rate was controlled at 0.15 nm s⁻¹ and 1 nm s⁻¹. It is well-known that thin film depositions on glass substrates are typically limited to anatase or anatase-rutile mixed phases due to the low melting point of most glasses. Therefore, the Ti coated ITO substrates were subsequently annealed at 300°C and/or 400°C for 8 h in air. The Ti coated silicon substrates were also annealed at 300°C, 400°C, 450°C and 700°C for 8 h in air. The deposition rate and annealing temperature of each samples are given in Table 1. The surface morphology of the samples was investigated using a Hitachi Field Emission Scanning Electron Microscopy (FE-SEM). The Ultraviolet-visible (UV-VIS) absorption spectra were measured using a Jasco UV-VIS-NIR V570 spectrometer and X-ray diffractograms were recorded on a XD-5000 diffractometer using CuK α radiation with wavelength of 1.5406 Å. In photoelectronic studies, a two-electrode photoelectrochemical cell was used. The cell is composed of ITO/TiO₂ used as the working electrode (the working area is 0.6 cm²) and a platinum electrode separated by an electrolyte containing 1 M KCl and 0.1 M Na₂S. The photocurrent was measured on an Auto-Lab Potentionstat PGS-30. A halogen lamp was used as the light source.

Table 1. Sample names at different deposition rate and annealing temperature.

Samples	Deposition rate (nm/s)	Annealing temperature (°C)
T1	0.15	350
T2	0.15	400
T3	0.15	450
T4	0.15	500
T5	0.15	700
T6	1.00	350
T7	1.00	400
T8	1.00	450

III. RESULTS AND DISCUSSION

1. Effect of deposition rate and annealing temperature on structural characterization of the TiO₂ thin films

Fig. 1.a shows the XRD patterns of samples a) T1, T2, T3, b) T4, T5, c) T6, T7, T8. As can be seen from Fig. 1.a, sample T1 (annealed temperature of 350°C), the titanium films were transformed to TiO₂. With an increase in annealing temperature up to 450°C (sample T3), the diffraction peaks at the 2 θ values of 25.21°; 37.80°; 48.04°; 53.80°; 55.06°; 62.61° correspond to the (101); (004); (200); (105); (211); (204) planes, respectively. According to the standard

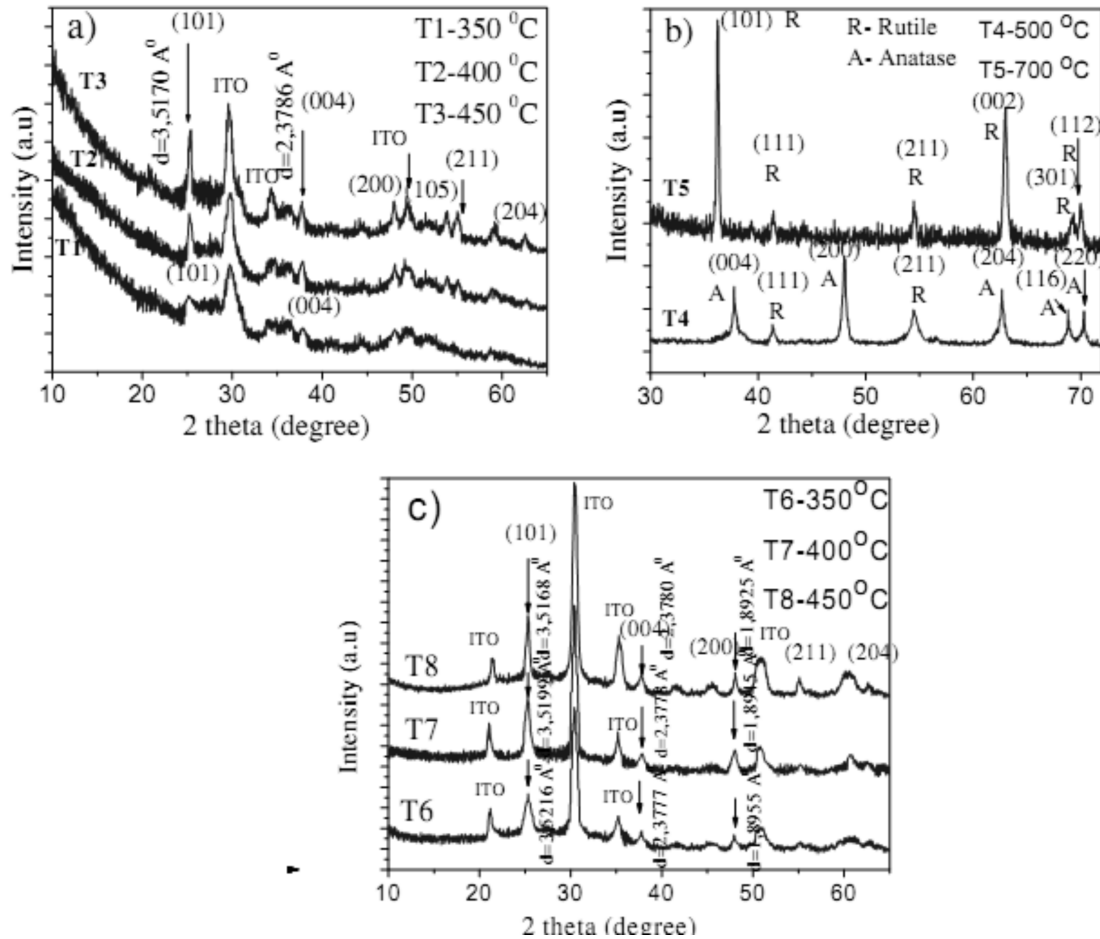


Fig. 1. XRD pattern of the samples a) T1, T2, T3, b) T4, T5 and c) T6, T7, T8

diffraction index (JCPDS 21-1272), these peaks are identified as anatase phase of TiO_2 . The anatase peaks in the spectra become more intense and sharp (samples named T2, T3 in Fig. 1.a, T7, T8 in Fig. 1.c). The increase in peak intensity with annealing temperature is due to an increase in crystallinity (crystal size) of the anatase phase. It is clear that the titanium films were completely transformed to TiO_2 and anatase phase occurs at heating treatment of 450°C . The XRD pattern of the sample T4 annealed at 500°C shows in Fig. 1.b). It can be observed that the anatase phase is the main phase. Diffraction peaks (111); (211) can be assigned to the planes of rutile phase. It is clear that at annealing temperature of 500°C , there is a small amount of rutile phase appeared in the sample. At annealing temperature of 700°C , the diffraction peaks at the 2θ values of 36.08° ; 41.3° ; 54.4° ; 63.0° ; 69.08° ; 69.8° correspond to the (101); (111); (211); (002); (301); (112) planes, respectively. According to the standard diffraction index (JCPDS 21-1276), these peaks are identified as rutile phase of TiO_2 . This result indicates the rutile phase is the dominating phase. No peaks corresponding to anatase phase were observed. The anatase phase transforms to rutile

phase completely at 700°C, which is lower than 900°C reported by Mathews *et al.* [12] and higher than 500°C reported by Hunsche *et al.* [9]

The average crystallite size of the TiO₂ thin films is estimated by the Scherrer's equation [19] as follows: $D = 0.89\lambda/\beta \cos \theta$, where D denotes the average crystallite size of the TiO₂ thin films, $\lambda = 0.15405$ nm is the X-ray wavelength of CuK α , β is the width of the peak measured at half maximum intensity (FWHM) and θ is the Bragg's angle of the peak. The crystallite size of the samples T1, T2, T3, T5, T6, T7, T8 are 15 nm, 25 nm, 34 nm, 60 nm, 12 nm, 17 nm, 20 nm, respectively. The crystallite size of the films increases with the annealing temperature. The lattice parameters were evaluated using the equation [4]: $\frac{1}{d_{hkl}^2} = \frac{h^2+k^2}{a^2} + \frac{l^2}{c^2}$ where d is the measured space of (hkl) planes, which is determined by Bragg's law. h, k, l are the Miller's indexes of crystalline plane relevant to the measured d -spacing. a and c are the lattice parameters of a tetragonal structure. The anatase phase has a tetragonal unit cell and the lattice parameters (a, c) can be calculated from the peak positions (101) and (004). The dependence of the lattice parameters on annealing temperature of samples T1, T2, T3, T6, T7, T8 are shown in Fig. 2.1) It can be observed that the lattice constant a decreases with the annealing temperature whereas the lattice constant c increases with temperature. Fig. 2.2 shows the dependence of ratio of lattice constant c/a on annealing temperature of samples T1, T2, T3 (deposition rate of 0.15 nm/s) and T6, T7, T8 (deposition rate of 1 nm/s). It can be seen that in the case of films annealed at 350°C (sample T6), 400°C (sample T7) the ratio c/a is closer to the bulk values of anatase phase than those of samples T1, T2. The ratio of lattice constant c/a increases to the bulk values of anatase phase (2.5133) with annealing temperature in both of deposition rates (0.15 nm/s and 1 nm/s). At annealing temperature of 450°C, the ratio c/a of all the samples reached to the value of bulk material. It is clear that when the annealing temperature is increased the strain decreased considerably. The decrease in strain indicates a decrease in lattice imperfections. This result agrees well with those of [12,20].

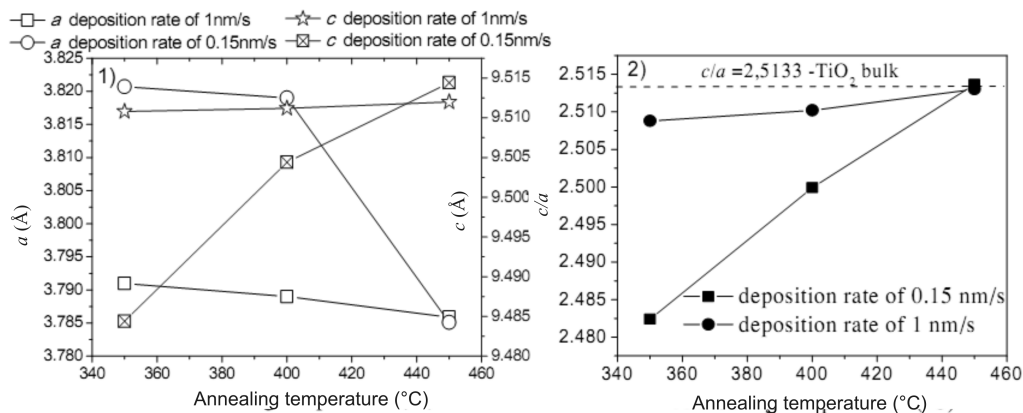


Fig. 2. 1) The dependence of lattice parameters on annealing temperature of the samples T1, T2, T3 and T6, T7, T8. 2) The dependence of ratio c/a on annealing temperature of the samples T1, T2, T3 and T6, T7, T8

2. Effect of deposition rate and annealing temperature on morphology of the TiO₂ thin films

Fig. 3 shows FE-SEM images of the annealed TiO₂ thin films (planar view) on silicon substrates at different temperatures. From the figure it is apparent that at annealing temperature of 350°C (sample T1 is not shown here), the TiO₂ thin film has a nanoparticle structure. The surface of the thin film is uniform and smooth with grain size less than 10 nm. The porous structure becomes visible after annealing at 400°C (sample T2). The average TiO₂ particle size was found to be less than 25 nm. The morphology and crystallinity are improved with increasing annealing temperature. It is clearly seen from the figure that at an annealing temperature of 450°C (sample T3), the TiO₂ thin film is uniform with grain size in the range of 30–35 nm. From the cross-sectional FE-SEM images of annealed TiO₂ thin films at 450°C (sample T3) and 700°C (sample T4), it can be seen that the length of the grains is from 300 nm to 400 nm. The TiO₂ rods are parallel to each other and probably perpendicular to the substrate. At an annealing temperature of 700°C, both the planar view and cross-sectional view show the agglomeration of grains with size of about 60 nm. The rod length completely occupied the thickness of the film. This result is the same with reported by Zhao *et al.* [21]. According to the report, TiO₂ anatase thin films obtained by magnetron sputtering have a nano-rod structure at annealed temperature under 500°C.

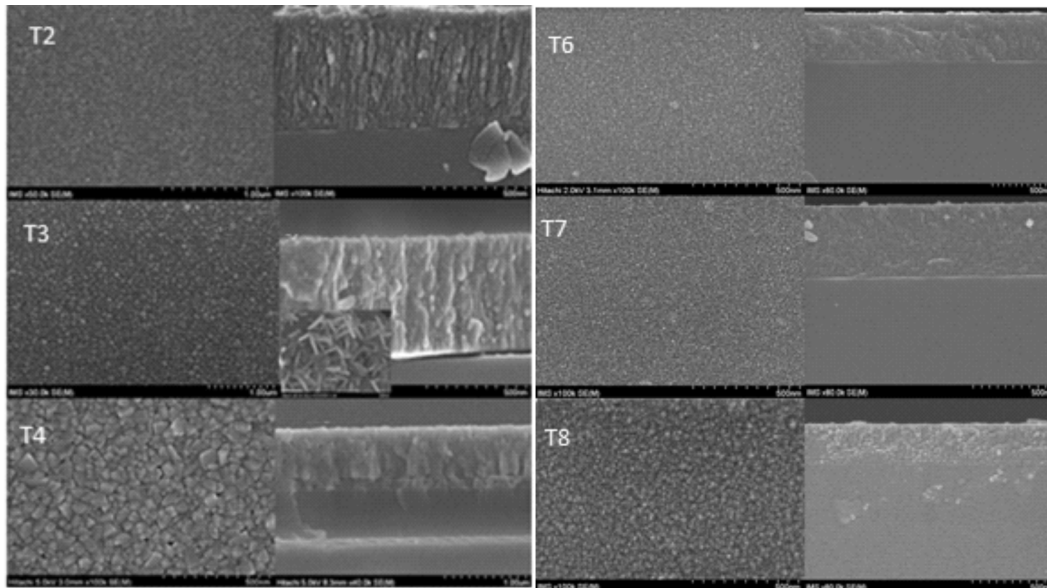


Fig. 3. FE-SEM images of surface and cross-section of samples T2, T3, T4 and T6, T7, T8

It is clear that Ti films deposited at a rate of 0.15 nm/s (samples T2, T3, T4) and an annealing temperature of 450°C, TiO₂ thin films obtained have a nanorod structure. This fact can be explained by taking into account that at low rate of deposition (0.15 nm/s), the Ti thin films are more dense. The outer Ti atoms will be oxidized to form TiO₂ first. The TiO₂ crystal nucleation will be facilitating the development of nanorod structure which is perpendicular to the substrate [18]. Furthermore, because of close-packed Ti thin films, the development of TiO₂ crystal formed during thermal oxidation is limited along orientation located on the thin film surface. Therefore,

only perpendicular orientation to the plane of the thin film is free. In contrast, at a deposition rate of 1 nm/s (samples T6, T7, T8), the Ti thin films obtained have more porosity. During thermal treatment process, oxygen atoms in the air easily diffuse into the pores between particles and oxidize Ti atoms to form TiO_2 . There are still gaps around the TiO_2 crystal formed which facilitate the development of nanoparticle structure, figure 3 (sample T8).

3. Optical characterization

The band gap energy of all the samples at different annealing temperature was calculated using the UV-Vis absorption spectra and Tauc formula [11]: $(\alpha d h\nu)^{1/2} = B(h\nu - E_g)$ where B is a constant, $h\nu$ is the photon energy, α is the absorption coefficient, d denotes film thickness. Figs. 4.1 and 4.2 present the extrapolating the straight line portion of the $[\alpha d(h\nu)]^{1/2}$ versus $h\nu$ plot for TiO_2 thin films at different annealing temperature. E_g is determined by the intersection between the tangent line of the graph with the horizontal axis (corresponding to the value of $\alpha = 0$). Fig. 4.3 shows the dependence of band gap energy of the samples on annealing temperature. It is clear that the band gap of TiO_2 thin films decreased with annealing temperature in both deposition rate of Ti thin films (For samples T1, T8, $E_g \sim 3.42$ eV, $E_g \sim 3.29$ eV, respectively).

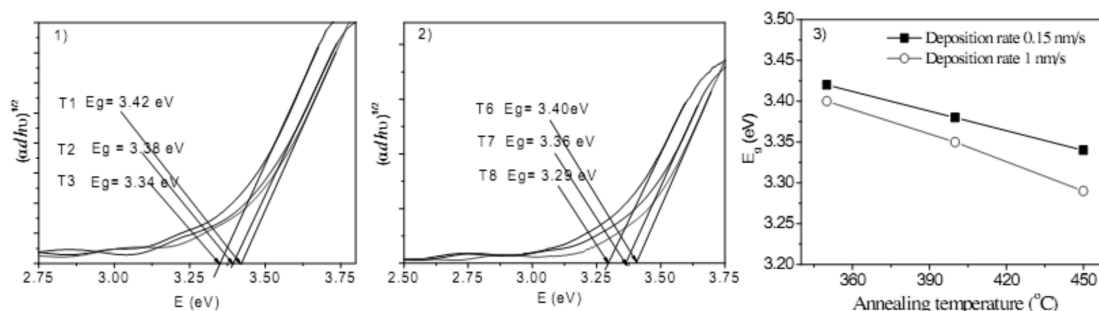


Fig. 4. The plots of $[\alpha d(h\nu)]^{1/2}$ versus $h\nu$ for TiO_2 thin films at different annealing temperature 1), 2) and the dependence of band gap energy of the samples on annealing temperature 3).

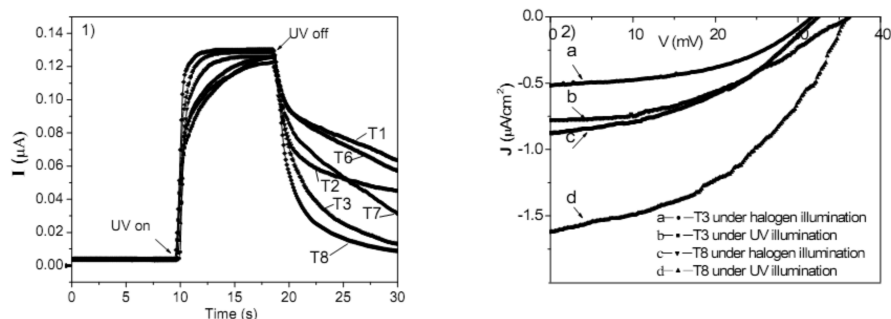


Fig. 5. 1) Photocurrent response of samples T1, T2, T3 and T6, T7, T8; 2) Photocurrent-potential behaviors of the ITO/ TiO_2 in turn under UV and halogen illumination.

The decrease in the optical band gap of TiO₂ films with annealing temperature might be the results of the change in film density and increase in grain size with decrease in strain of the film [12, 20]. This result is consistent with previous studies [2, 5, 8, 10–12, 21].

4. Effect of annealing temperature on photoresponse and photoelectronic performance of TiO₂ thin films

Prior to the measurement, the film with two parallel electrical contacts were kept in dark for 30 min to stabilize the current at a applied potential of 1V. After the stabilization period the current was captured at each second in the following sequence: 10s in dark, 10s under UV illumination, and finally 10s in dark. The photoresponse of TiO₂ films annealed at different temperatures are presented in figure 5.1. It can be observed that for the samples annealed at 350°C (T1, T6) show a slow rise in the photocurrent under UV illumination and a slow decay in the dark. In contrast, the response of the films annealed at 450°C (samples T3, T6) presented a faster rise and fall in photocurrent under UV on and off, respectively. The slow rise of photocurrent indicates trapping of the photo-generated carriers at trap states caused by the defects in the structure of TiO₂ films, and the slow decay in dark is due to the thermal de-trapping of the trapped carriers. The faster rise and fall predicts that a better recrystallization reduces the density of trap states [12].

Fig. 5.2 shows the photocurrent-potential behaviors of the photo-electrochemical cell with ITO/TiO₂ (TiO₂ was the sample with deposition rate of 0.15 nm/s, at an annealing temperature of 450°C-T3 and the sample with deposition rate of 1nm/s, at an annealing temperature of 450°C-T8) used as working electrodes in turn under UV and halogen illumination. The open-circuit photovoltage (V_{OC}) and the short-circuit photocurrent (J_{SC}) are given in Table 2. As can be seen from the table that the photo-electrochemical cell with working electrode made of sample T3 has low value for V_{OC} and J_{SC} , whereas in sample T8, both V_{OC} and J_{SC} increase significantly. This can be explained as follows: Although sample T3 has a nanorod-structure but high density of nanorod and smooth surface. In contrast, sample T8 has higher porosity, therefore the area of contact between the TiO₂ surface with an electrolyte is higher than the case of sample T3. That ameliorates the charge exchange process at sample T8 leading to an increase in short circuit photocurrent. On the other hand, the optical band gap of sample T8 (3.29 eV) is lower than that of sample T3 (3.34 eV). This also contributes to the ability of sample T8 to absorb light.

Table 2. The open-circuit photovoltage (V_{OC}) and the short-circuit photocurrent (J_{SC}) of sample T3 and T8 used as working electrodes in turn under UV and halogen illumination

Illumination sources	Sample T3		Sample T8	
	V_{OC} (mV)	J_{SC} ($\mu\text{A}/\text{cm}^2$)	V_{OC} (mV)	J_{SC} ($\mu\text{A}/\text{cm}^2$)
halogen	32	0.5	36	0.8
UV	34	0.9	37	1.6

IV. CONCLUSIONS

TiO₂ thin films have been successfully prepared by an EBD method combined with thermal process. At the same an annealing temperature of 450 °C, the TiO₂ films with a deposition rate of

0.15 nm/s of Ti thin films have a nanorod structure. The length of the grains is from 300 nm to 400 nm. The TiO₂ rods are parallel to each other and probably perpendicular to the substrate. In contrast, at a deposition rate of 1 nm/s of Ti thin films, the porous structure appeared with particle size less than 20 nm. The transform from anatase to rutile phase begins at 500°C and completes at 700°C. At annealing temperature of 450°C, all the samples consist of quite pure anatase TiO₂. The band gap of TiO₂ thin films decreased with annealing temperature in both deposition rate of Ti thin films. The response of the films annealed at 450°C (samples T3, T6) exhibits a faster rise and fall of photocurrent.

ACKNOWLEDGMENTS

This work is supported in part by the Science and Technology Research Projects of Vietnam Academy of Science and Technology, the project, code: VAST03.05/13-14. A part of the work was done with the help of the Key Laboratory in Electronic Materials and Devices, Institute of Materials Science, Vietnam Academy of Science and Technology. We would like to thank the colleagues for their contribution to the work.

REFERENCES

- [1] P. C. A. Alberius, K. L. Frindell, R. C. Hayward, E. J. Kramer, G. D. Stucky, and B. F. Chmelka, *Chemistry of Materials* **14** (2002) 3284-3294.
- [2] L. Castañeda, J. C. Alonso, A. Ortiz, E. Andrade, J. M. Saniger, and J. G. Bañuelos, *Materials Chemistry and Physics* **77** (2003) 938-944.
- [3] A. Conde-Gallardo, M. Guerrero, N. Castillo, A. B. Soto, R. Fragoso, and J. G. Cabañas-Moreno, *Thin Solid Films* **473** (2005) 68-73.
- [4] B. D. Cullity, *Elements of X-Ray Diffraction*, Wesley Pub, Note Dame (1978).
- [5] N. N. Dinh, N. T. Oanh, and P. D. Long, *Advances in Natural Sciences* **2** (2001) 3-11.
- [6] Q. Fan, B. McQuillin, D. D. C. Bradley, S. Whitelegg, and A. B. Seddon, *Chemical Physics Letters* **347** (2001) 325-330.
- [7] T. Fujii, N. Sakata, J. Takada, Y. Miura, Y. Daitoh, and M. Takano, *Journal of Materials Research* **9** (1994) 1468-1473.
- [8] L. Ge, M. Xu, and H. Fang, *Thin Solid Films* **515** (2007) 3414-3420.
- [9] B. Hunsche, M. Verghl, and A. Ritz, *Thin Solid Films* **502** (2006) 188-192.
- [10] G. X. Liu, F. K. Shan, W. J. Lee, and B. C. Shin, *Journal of the Korean Physical Society* **50** (2007) 1827-1832.
- [11] D. Mardare and G. I. Rusu, *Materials Letters* **56** (2002) 210-214.
- [12] N. R. Mathews, E. R. Morales, M. A. Cortés-Jacome, and J. A. Toledo Antonio, *Solar Energy* **83** (2009) 1499-1508.
- [13] C. B. Murray, D. J. Noms, and M. G. Bawendi, *J. Am. Chem. Soc.* **115** (1993) 8706-8715.
- [14] B. O'Regan and M. Grätzel, *Nature* **353** (1991) 737-740.
- [15] J. Rodríguez, M. Gómez, J. Lu, E. Olsson, and C. G. Granqvist, *Advanced Materials* **12** (2000) 341-343.
- [16] G. Shukla, P. K. Mishra, and A. Khare, *Journal of Alloys and Compounds* **489** (2010) 246-251.
- [17] R. Tang, W. Zhang, and Y. Li, *Journal of Alloys and Compounds* **496** (2010) 380-384.
- [18] Dang Tran Chien, Pham Duy Long, Le Ha Chi, and Pham Van Hoi, *Advances in Natural Sciences: Nanoscience and Nanotechnology* **1** (2010) 015002.
- [19] M. C. Wang, H. J. Lin, and T. S. Yang, *Journal of Alloys and Compounds* **473** (2009) 394-400.
- [20] B. Yarmand and S. K. Sadrezaad, *Journal of Optoelectronics and Advanced Materials* **12** (2010) 1490 - 1497.
- [21] B. Zhao, J. Zhou, Y. Chen, and Y. Peng, *Journal of Alloys and Compounds* **509** (2011) 4060-4064.